

INFLUENCE OF THE MODULATION METHOD ON THE CONDUCTION
AND SWITCHING LOSSES OF A PWM CONVERTER SYSTEM

JOHANN W. KOLAR, HANS ERTL, FRANZ C. ZACH
Technical University Vienna, Power Electronics Section, Gußhausstraße 27,
Vienna, AUSTRIA

Phone: (int)43 222 58801-3886 Fax: (int)43 222 5052666

Abstract

The optimization of the modulation method of a PWM converter system in general leads to not purely sinusoidal phase modulation functions. In connection with the output currents and the forward characteristics of the electric valves these phase modulation functions define directly the conduction losses of the power electronic devices. This paper explores the dependency of the conduction losses of a bridge leg of a PWM converter system with high pulse rate on the shape of the phase modulation functions. This is done for modulation methods which are optimized with respect to minimum harmonic current rms values. The results are compared to the results gained for simple sinusoidal modulation.

Besides the conduction losses furthermore the switching losses of the electric valves are calculated. Deviations from the classical sinusoidal modulation here are only obtained for modulation methods for which the output voltage is formed by a cyclic change via only two active and a third, not switching bridge leg. As the calculations show, these modulation methods allow a significant increase of the effective switching frequency. This effect is dependent on the phase angle between the fundamental of the converter output phase voltage and the converter output phase current; for this comparison equal switching losses as for the simple sinusoidal modulation are assumed.

In conclusion the optimal modulation of the pulse frequency of a PWM converter system is treated. There a side condition has to be observed stating that the switching power loss has to correspond to the power loss occurring for operation with constant pulse frequency. The optimal modulation as calculated leads to a reduction of the harmonic power loss in the upper modulation region. Furthermore, due to the frequency modulation the spectrum is spread out to a wider frequency band as compared to the operation with constant pulse frequency; there the spectrum is concentrated to harmonics in the vicinity of multiples of the pulse frequency. This effect can influence the noise generation of, e.g., a motor supplied by a converter.

Keywords: PWM Converter System, Pulse Pattern Optimization, Conduction Losses, Switching Losses, Phase Modulation Function, Optimal Frequency Modulation

1 Introduction

In this section we want to briefly summarize these modulation methods which will be applied in the subsequent calculations. For their characterization the resulting harmonic power losses and the shape of the phase modulation func-

tions are used. Attention is paid especially to the correspondence of the description of the voltage formation using space vector calculus and representation by phase quantities. This is of special importance here because the determination of conduction and switching losses (which can be linked to a certain modulation method) of a PWM converter system (cf. Fig.1) corresponds directly to phase quantities (phase currents or phase modulation functions); furthermore, the optimization of the frequency modulation (which is discussed at the end of this paper) is essentially connected to a description of the system quantities by space vectors. The definition of the converter voltage space vector is given by

$$\underline{u}_U = \frac{2}{3} [u_{U,R} + \underline{a} u_{U,S} + \underline{a}^2 u_{U,T}] \quad \underline{a} = \left(-\frac{1}{2} + j\frac{\sqrt{3}}{2}\right) \quad (1)$$

If purely sinusoidal converter output voltage is postulated according to

$$\underline{u}_U^* = \hat{U}_U^* \exp j\varphi_U \quad \varphi_U = \omega_N \tau \quad (2)$$

the control signals for the power semiconductor devices can be derived in the simplest case as shown in Fig.2 by "sampling" of sinusoidal phase modulation functions

$$\begin{aligned} m'_R(\varphi_U) &= M \cos \varphi_U \\ m'_S(\varphi_U) &= M \cos \left(\varphi_U - \frac{2\pi}{3}\right) \\ m'_T(\varphi_U) &= M \cos \left(\varphi_U + \frac{2\pi}{3}\right) \end{aligned} \quad (3)$$

with

$$M = \frac{2\hat{U}_{U,(1)}}{U_{ZK}} = \frac{2\hat{U}_U^*}{U_{ZK}} = M_{(1)} = M_1 \quad M \in [0,1] \quad (4)$$

(cf. Fig.3). The angle φ_U (or time τ) denotes the position of the resulting converter voltage space vector or the position of the corresponding pulse interval within the fundamental period. There the considerations are limited to the treatment of the voltage fundamental or to the average value for one pulse period or for half a pulse period. One full pulse period is used for symmetric regular sampling, half a pulse period is used for asymmetric regular sampling (cf. Ref.[1]). This distinction is not important here, however, due to the high pulse rate assumed.

This method (known as *subharmonic modulation*) leads to relative turn-on times (related to the pulse period) of the converter bridge legs (which can

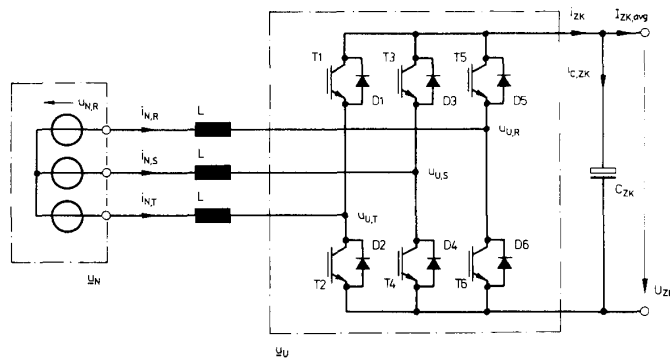


Fig.1: Structure of the power circuit of a three-phase voltage DC link PWM converter system. For usage as *PWM inverter* for AC machine drives the inductances L and the three phase system \underline{u}_N can be interpreted as simple equivalent circuit of the AC machine formed by leakage inductances and machine counter emf. On the other hand, for mains operation of the *PWM converter* (PWM rectifier, static VAR compensator) the inductances have to be connected in series; the voltage system \underline{u}_N is defined by the mains conditions.

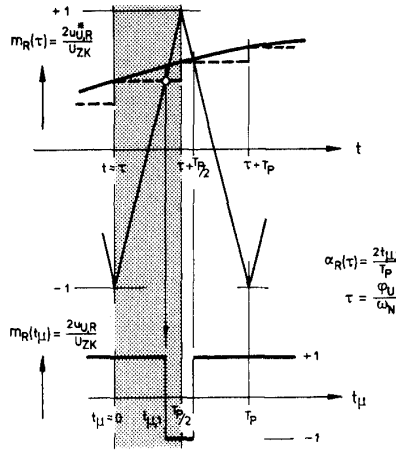


Fig. 2: Derivation of the switching times of a converter bridge leg via intersection of the relevant phase modulation function with a triangular signal (shown for asymmetric regular sampling).

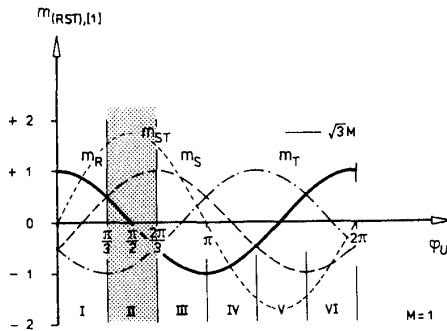
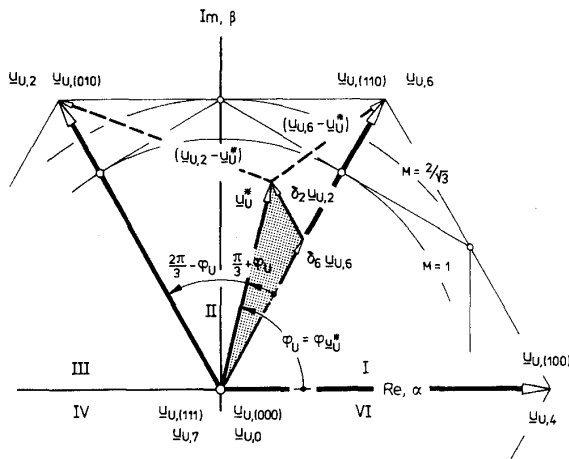


Fig. 3: Shape of the phase modulation functions for the classical sinusoidal modulation (denoted by [1] in this paper).



be replaced by three double-pole switches between positive and negative DC link voltage bus regarding their electrical function) according to

$$\begin{aligned} \alpha_R(\varphi_U) &= \frac{1}{2}[1 + m_R(\varphi_U)] \\ \alpha_S(\varphi_U) &= \frac{1}{2}[1 + m_S(\varphi_U)] \\ \alpha_T(\varphi_U) &= \frac{1}{2}[1 + m_T(\varphi_U)] \end{aligned} \quad (5)$$

Due to the symmetries of the generated voltage system resulting from the three-phase properties the further considerations can be limited to the interval of the angle

$$\varphi_U \in \left[\frac{\pi}{3}, \frac{2\pi}{3} \right] \quad (6)$$

By introduction of space vector calculus the relative turn-on times of the bridge legs given by Eq.(5) can be described as a weighting (with respect to time)

$$\begin{aligned} \delta_7 &= \alpha_T \\ \delta_6 &= (\alpha_R - \alpha_T) \\ \delta_2 &= (\alpha_S - \alpha_R) \\ \delta_0 &= (1 - \alpha_S) \end{aligned} \quad (7)$$

of the voltage space vectors $\psi_{U,7}$, $\psi_{U,6}$, $\psi_{U,2}$ and $\psi_{U,0}$, which are associated to the switching states of the PWM converter (cf. Fig. 4). The indices denote the converter switching state by the decimal equivalent of the converter switching status vector interpreted as binary number. Therefore Eqs.(7) define the transition of a description by phase quantities to a description by space vector calculus. The modulation method is characterized by the switching state sequence

$$\varphi_U \in \left[\frac{\pi}{3}, \frac{2\pi}{3} \right] \quad \dots 0 2 6 7 \Big|_{t_\mu=0} 7 6 2 0 \Big|_{t_\mu=\frac{T_p}{2}} 0 2 6 7 \dots ; \quad (8)$$

this sequence in general is denoted as {7620}. The transition between two subsequent switching states there is always achieved by switching of only one bridge leg.

In the space vector representation of the converter voltage the two not voltage forming switching states 0 and 7 cannot be distinguished. Therefore, for definition of the converter output voltage by space vector calculus only the entire free-wheeling state period

$$\delta_0 + \delta_7 = 1 - (\delta_2 + \delta_6) \quad (9)$$

can be given. The voltage formation of the converter system (related to the average value for one pulse period T_p) is not influenced by the distribution of the free-wheeling states within the pulse interval. The definition of a particular distribution of free-wheeling states is really the ultimate basis for the definition of phase modulation functions (cf. Eq.(7)). The degree of freedom given thereby can now be applied for the optimization of the modulation method. The quality functional to be minimized shall be defined as the squared rms value of the resulting current harmonics:

$$\begin{aligned} I &= \Delta I_{N,rms}^2 = \\ &= \frac{1}{3T_N} \int_{T_N} \left\{ \frac{2}{T_p} \int_{t_\mu=0}^{t_\mu=\frac{T_p}{2}} (\Delta i_{N,R}^2 + \Delta i_{N,S}^2 + \Delta i_{N,T}^2) dt_\mu \right\} d\tau \\ &= \frac{1}{3T_N} \int_{T_N} \Delta i_{N,RST,rms}^2(\tau) d\tau \rightarrow Min \end{aligned} \quad (10)$$

Fig. 4: Approximation of the reference value of the output voltage space vector via neighbouring converter voltage space vectors (due to the 60°-symmetry of the voltage space vectors following for the different converter switching states one can limit the considerations to the interval of $\varphi_U \in [\pi/3, 2\pi/3]$ shown here).

Equation (10) is obtained with good approximation for PWM converter systems with high pulse rate (Ref.[2]). For the deviation of the current space vector

$$\Delta \dot{i}_N = \dot{i}_N - \dot{i}_N^* \quad (11)$$

from that of a purely sinusoidal three-phase system

$$\dot{i}_N^*(\tau) = \hat{I}_N \exp j(\omega_N \tau + \varphi) \quad \varphi = \varphi_{u_V, \dot{i}_N^*} \quad (12)$$

we have

$$\frac{d\Delta \dot{i}_N}{dt_\mu} = \frac{1}{L} [\dot{u}_V^*(\tau) - u_V(\tau, t_\mu)] \quad (13)$$

(cf. Ref.[2]) and

$$\Delta i_{N,R}^2 + \Delta i_{N,S}^2 + \Delta i_{N,T}^2 = \frac{3}{2} |\Delta \dot{i}_N|^2 \quad (14)$$

The minimization of the quality functional I leads to

$$\Delta i_{N,RST,rms}^2(\tau) \rightarrow Min. \quad (15)$$

There, $\Delta i_{N,RST,rms}^2$ characterizes a "local" (related to a pulse interval) harmonic power loss contribution. It can be set equal to the square of a local harmonic current rms value. It shows the dependency given by

$$\begin{aligned} \Delta i_{N,RST,rms}^2(\tau) &= \Delta i_{N,RST,rms,1}^2 \{ \delta_7(\tau), \delta_6(\tau), \delta_2(\tau) \} + \\ &+ \Delta i_{N,RST,rms,2}^2 \{ \delta_6(\tau), \delta_2(\tau) \} \end{aligned} \quad (16)$$

on the weighting (with respect) to time of the different converter voltage space vectors. The optimal phase modulation functions follow (as, e.g., discussed also in Ref.[3]) as

$$\begin{aligned} m_R(\varphi_U) &= M_1 \cos \varphi_U - M_3 \cos 3\varphi_U \\ m_S(\varphi_U) &= M_1 \cos \left(\varphi_U - \frac{2\pi}{3} \right) - M_3 \cos 3\varphi_U \\ m_T(\varphi_U) &= M_1 \cos \left(\varphi_U + \frac{2\pi}{3} \right) - M_3 \cos 3\varphi_U \end{aligned} \quad (17)$$

with

$$\left. \frac{M_3}{M_1} \right|_{I=\min} = \frac{1}{4}; \quad M_3 = \frac{2\hat{U}_{U,(3)}}{U_{ZK}} \left(M_{1,max} \left| \frac{M_3}{M_1} \right|_{\frac{M_3}{M_1}=\frac{1}{4}} = 0.972 \frac{2}{\sqrt{3}} \right) \quad (18)$$

The corresponding phase modulation functions are shown in Fig.5 (cf. [3]¹). For the global (as related to the fundamental period) harmonic current rms value then we have in general with Eqs.(15), (16) and (10)

$$\Delta I_{N,rms,[3]}^2 = \frac{1}{6} \Delta i_n^2 M_1^2 \left\{ 1 - \frac{8M_1}{\sqrt{3}\pi} + \frac{3M_1^2}{4} \left[1 - \frac{M_3}{M_1} \left(1 - 2 \frac{M_3}{M_1} \right) \right] \right\} \quad (19)$$

with

$$\Delta i_n = \frac{U_{ZK} T_P}{8L} \quad (20)$$

(cf. [3] in Fig.6). The maximum modulation region

$$M \in \left[0, \frac{2}{\sqrt{3}} \right] \quad (21)$$

follows for $M_3/M_1 = 1/6$ (cf. Ref.[2] and Ref.[4]).

A simple suboptimal approximation (denoted by [2] in this paper) can be given by distributing the free-wheeling state to equal parts at the beginning and at the end of each pulse half interval according to

$$\delta_{7,[2]} = \frac{1}{2} (\delta_0 + \delta_7) = \frac{1}{2} [1 - (\delta_2 + \delta_6)] \quad (22)$$

(cf. Ref.[2] and Ref.[5]). For the global harmonic rms value there follows

$$\Delta I_{N,rms,[2]}^2 = \frac{1}{6} \Delta i_n^2 M^2 \left[1 - \frac{8M}{\sqrt{3}\pi} + \frac{9M^2}{8} \left(1 - \frac{3\sqrt{3}}{4\pi} \right) \right] \quad M \in \left[0, \frac{2}{\sqrt{3}} \right] \quad (23)$$

As already mentioned, for a simple sinusoidal modulation (denoted by [1]) the distribution of the free-wheeling states is determined directly by the shape

of the phase modulation functions. It follows as

$$\delta_{7,[1]} = \frac{1}{2} + \frac{M}{2} \cos(\varphi_U + \frac{2\pi}{3}) \quad (24)$$

In this case we have for the global harmonic rms value

$$\Delta I_{N,rms,[1]}^2 = \frac{1}{6} \Delta i_n^2 M^2 \left[1 - \frac{8M}{\sqrt{3}\pi} + \frac{3M^2}{4} \right] \quad M \in [0, 1] \quad (25)$$

As a limiting case of the distribution of the free-wheeling states as discussed, also a formation of the switching state sequence according to

$$\begin{aligned} \delta_7 &= 1 - (\delta_2 + \delta_6) \\ \delta_0 &= 0 \end{aligned} \quad (26)$$

$$\dots 2 \ 6 \ 7 \Big|_{t_\mu=0} \ 7 \ 6 \ 2 \Big|_{t_\mu=T_P/2} \ 2 \ 6 \ 7 \dots \quad \{762\} \text{ or } [6] \quad (27)$$

or

$$\begin{aligned} \delta_7 &= 0 \\ \delta_0 &= 1 - (\delta_2 + \delta_6) \end{aligned} \quad (28)$$

$$\dots 0 \ 2 \ 6 \Big|_{t_\mu=0} \ 6 \ 2 \ 0 \Big|_{t_\mu=T_P/2} \ 0 \ 2 \ 6 \dots \quad \{620\} \text{ or } [7] \quad (29)$$

can be considered. There the entire free-wheeling state is concentrated at the beginning or at the end of a pulse half interval. Due to the then given not optimal "distribution" there result higher harmonic losses of the system, however. The analysis of the associated phase modulation functions (cf. [6] and [7] in Fig.5) shows, however, that then the output voltage system is formed by pulsing of only two bridge legs, whereas the third phase remains "clamped" to one of the two DC link voltage bus bars ("discontinuous modulation"). Accordingly the conclusion is obvious that an increase of the pulse frequency by a factor $k_f = 3/2$ leads to equal switching losses and equal thermal stress to the power semiconductor devices as compared to the case of "continuous modulation" (modulation function without discontinuities, or, equivalent, pulsing of always all bridge legs as used for methods [1], [2], [3]). A closer investigation shows, however, that the possible frequency increase is determined essentially by the phase relationship between output current fundamental and output voltage fundamental. This aspect is treated in section 3 in detail. The harmonic losses resulting for the modulation methods given by Eqs.(26) and (28) (or Eqs.(27) and (29), respectively) follow as

$$\Delta I_{N,rms,[6],[7]}^2 = \frac{1}{6} \Delta i_n^2 M^2 \frac{1}{k_{f,[6],[7]}^2} \left[4 - \frac{35M}{\sqrt{3}\pi} + \frac{9M^2}{8} \left(2 + \frac{3\sqrt{3}}{4\pi} \right) \right] \quad M \in \left[0, \frac{2}{\sqrt{3}} \right] \quad (30)$$

They are shown in Fig.6 (cf. [6] and [7]) for $k_{f,[6],[7]} = 3/2$. The possible frequency increase therefore leads to a significant harmonic power loss reduction in the upper modulation region, also if compared to optimal continuous modulation.

For a combination (denoted by [4]) of the switching state sequences (given by Eqs.(27) and (29)) according to

$$\begin{aligned} \{762\} &\quad \text{for} \quad \varphi_U \in \left[\frac{\pi}{3}, \frac{\pi}{2} \right] \\ \{620\} &\quad \text{for} \quad \varphi_U \in \left[\frac{\pi}{2}, \frac{2\pi}{3} \right] \end{aligned} \quad (31)$$

there follows

$$\Delta I_{N,rms,[4]}^2 = \frac{1}{6} \Delta i_n^2 M^2 \frac{1}{k_{f,[4]}^2} \left[4 - \frac{M}{\sqrt{3}\pi} (62 - 15\sqrt{3}) + \frac{9M^2}{8} \left(2 + \frac{\sqrt{3}}{\pi} \right) \right] \quad M \in \left[0, \frac{2}{\sqrt{3}} \right] \quad (32)$$

(cf. [4] in Figs.5, 6).

An alternative combination (denoted by [5])

$$\begin{aligned} \{620\} &\quad \text{for} \quad \varphi_U \in \left[\frac{\pi}{3}, \frac{\pi}{2} \right] \\ \{762\} &\quad \text{for} \quad \varphi_U \in \left[\frac{\pi}{2}, \frac{2\pi}{3} \right] \end{aligned} \quad (33)$$

leads to

¹By brackets here we denote modulation methods (e.g., in Fig.5); references are given by, e.g., "Ref.[1]"

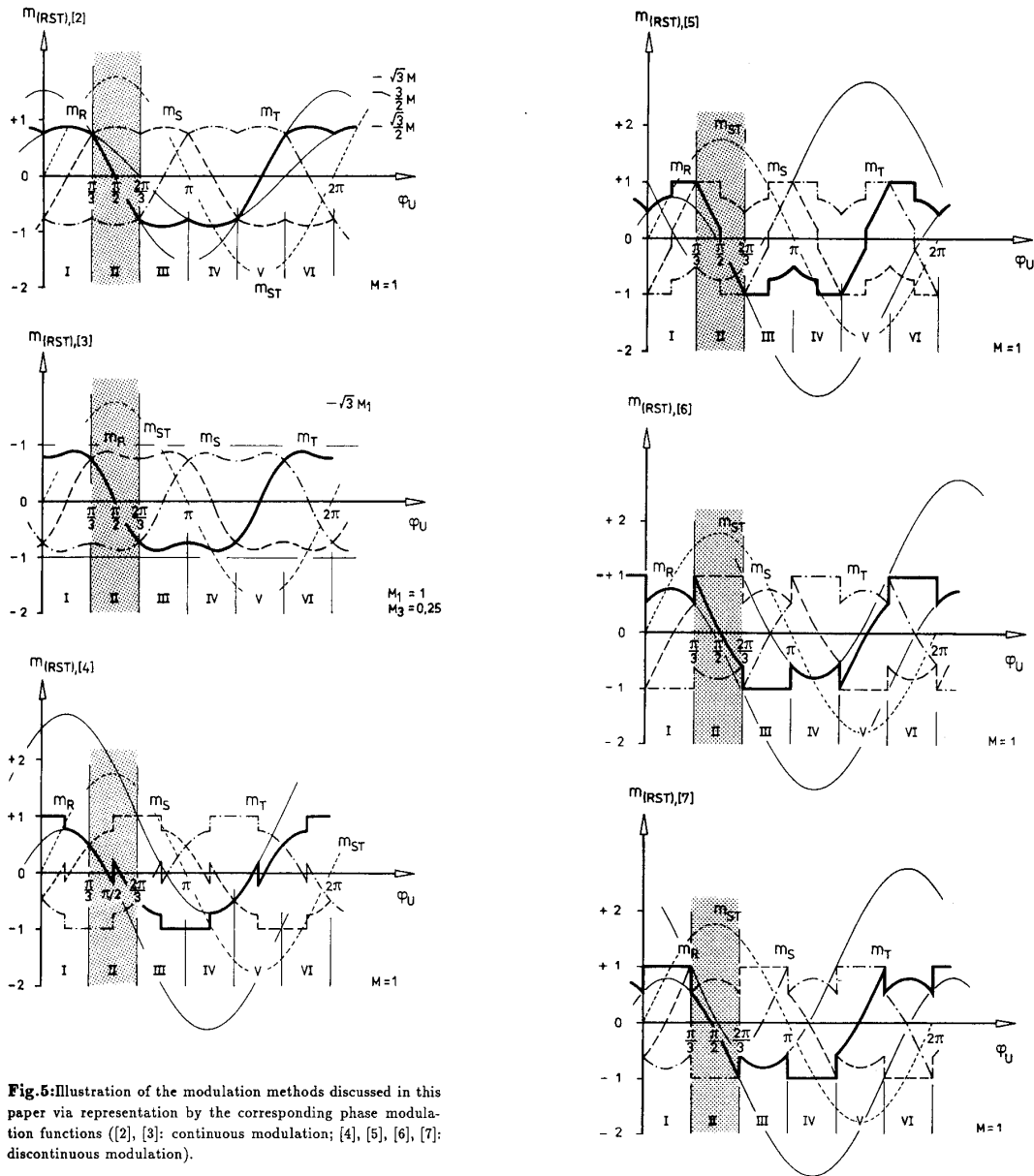


Fig.5: Illustration of the modulation methods discussed in this paper via representation by the corresponding phase modulation functions ([2], [3]: continuous modulation; [4], [5], [6], [7]: discontinuous modulation).

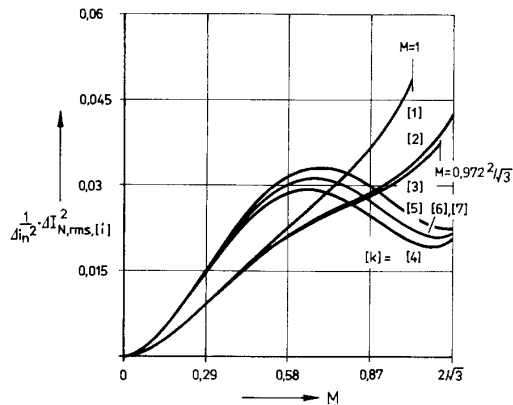


Fig.6: Comparison of the normalized harmonic power losses of one phase for various modulation methods (discussed in section 1); [1]: Sinusoidal modulation (Eq.(25)); [2]: Suboptimal space vector modulation (Eq.(23)); [3]: Local and global optimal sinusoidal modulation with added third harmonic ($M_3 = M_1/4$, Eq.(19)); [4],[5],[6],[7]: Discontinuous modulation (cf. Eqs.(30, 32, 34)); $k_{f,[4],[5],[6],[7]} = 3/2$.

$$\Delta I_{N,rms,[5]}^2 = \frac{1}{6} \Delta i_n^2 M^2 \frac{1}{k_f^2 [5]} \left[4 - \frac{M}{\sqrt{3}\pi} (8 + 15\sqrt{3}) + \frac{9M^2}{8} \left(2 + \frac{\sqrt{3}}{2\pi} \right) \right] \quad (34)$$

$$M \in \left[0, \frac{2}{\sqrt{3}} \right]$$

(cf. [5] in Figs.5, 6). Equation (31) in this way defines based on a possible frequency increase $k_f = 3/2$ the harmonic-optimal discontinuous modulation method (cf. [4], [5], [6], [7] in Fig.6, see also Ref.[2]).

Finally we want to point out that all the modulation functions discussed here can be derived by extension of a simple sinusoidal modulation according to

$$\begin{aligned} m_R &= m'_R + m_0 \\ m_S &= m'_S + m_0 \\ m_T &= m'_T + m_0 \\ m_0 &= \frac{1}{3} (m_R + m_S + m_T) \end{aligned} \quad (35)$$

The zero quantity m_0 is not projected into the corresponding space vector when the voltage system is transformed (the zero voltage is decoupled); m_0 only influences the distribution of the free-wheeling states and therefore the resulting harmonic losses.

2 Calculation of the Conduction Losses of the Power Semiconductor Devices

The relative conduction periods of the power electronic devices of the bridge legs within a pulse half period are defined (as mentioned in the introduction) according to

$$\begin{aligned} \alpha_{T2}(\varphi_U) &= \alpha_R(\varphi_U) \\ \alpha_{D1}(\varphi_U) &= 1 - \alpha_R(\varphi_U) \end{aligned} \quad \text{with } \varphi_U = \omega_N \tau \quad (36)$$

(given for phase R and limited to the positive current half period; cf. Fig.7) directly by the shape of the phase modulation functions. If one approximates the forward characteristic of the valves by

$$u_{F,Ti,Di} = U_{F,T,D} + r_{F,T,D} i_{Ti,Di} \quad (37)$$

there follows for the mean value of the conduction losses within one pulse half period ("local" conduction losses, i.e. "local" with respect to time)

$$\begin{aligned} P_{F,T2}(\tau) &= U_{F,T} i_{T2,avg}(\tau) + r_{F,T} i_{T2,rms}^2(\tau) \\ &= U_{F,T} \alpha_R(\tau) i_{T2}(\tau) + r_{F,T} \alpha_R(\tau) i_{T2}^2(\tau) \end{aligned} \quad (38)$$

with

$$i_{T2}(\tau) = i_{N,R}(\tau) = \hat{I}_N \cos(\omega_N \tau + \varphi) \quad (39)$$

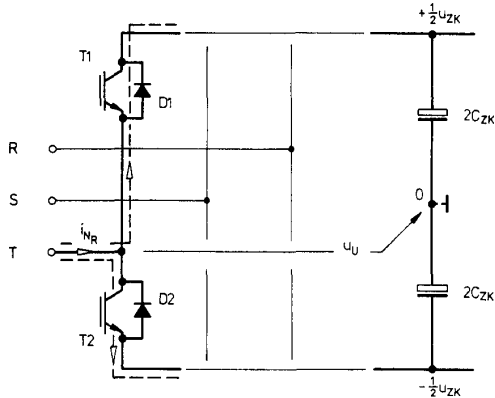


Fig. 7: Division of the output current flowing into controlled and uncontrolled semiconductor devices of a PWM converter bridge leg.

The integration of these local conduction losses for the positive (or negative) half cycle of the output current

$$\begin{aligned} P_{F,T2} &= U_{F,T} \left\{ \frac{1}{T_N} \int_{-\pi/2-\varphi}^{\pi/2-\varphi} \frac{\omega_N}{\omega_N} \alpha_R(\tau) i_{T2}(\tau) d\tau \right\} + \\ &+ r_{F,T} \left\{ \frac{1}{T_N} \int_{-\pi/2-\varphi}^{\pi/2-\varphi} \frac{\omega_N}{\omega_N} \alpha_R(\tau) i_{T2}^2(\tau) d\tau \right\} \end{aligned} \quad (40)$$

finally leads to

$$P_{F,T2} = \frac{U_{F,T} \hat{I}_N}{2} \left[\frac{1}{\pi} + \frac{M}{4} \cos \varphi \right] + r_{F,T} \hat{I}_N^2 \left[\frac{1}{8} + \frac{M}{3\pi} \cos \varphi \right] \quad (41)$$

for the global (i.e., related to the fundamental period) conduction loss. There simple sinusoidal modulation

$$\alpha_R(\tau) = \frac{1}{2} [1 + M \cos \omega_N \tau] \quad (42)$$

is assumed. Integration for the output current half cycle therefore means integration of a quantity $\alpha_{T2}(\tau)$ (or $\alpha_{D1}(\tau)$) which is weighted by the instantaneous current value (and dependent on the position φ_U of the converter voltage space vector) within an interval which is dependent on the phase angle between the fundamentals of the converter output phase voltage and current. For the conduction losses of the diode which conducts current for positive output current there follows then (cf. also Refs.[6,7,8])

$$P_{F,D1} = \frac{U_{F,D} \hat{I}_N}{2} \left[\frac{1}{\pi} - \frac{M}{4} \cos \varphi \right] + r_{F,D} \hat{I}_N^2 \left[\frac{1}{8} - \frac{M}{3\pi} \cos \varphi \right] \quad (43)$$

The purely sinusoidal output current shape being assumed by Eq.(39) limits together with Eq.(38) the validity of Eq.(41) or Eq.(43), respectively, to a region of high pulse numbers pz (ratio of the pulse frequency to the output frequency). It can be used, however, (as a comparison with the results of a digital simulation shows) in practice already for $pz > 21$ with sufficient accuracy for the thermal dimensioning of the valves. One has to mention in general that dimensioning on the basis of *global* power losses (i.e., averaged over the fundamental period) assumes sufficient (i.e., sufficient for the time of averaging applied, i.e., for the fundamental period) thermal inertia of the power semiconductors. This assumption is sufficiently well fulfilled for pulse rectifier systems for high power (the averaging time is given by the mains fundamental period). For converters used in drives the validity of the relationships derived in this paper is limited to the higher frequency or modulation region. (There, approximately frequency-proportional change of the output voltage amplitude is usually given.) For low output frequencies, *local* power losses have to be considered for dimensioning.

If the simple sinusoidal modulation is extended by addition of a third harmonic Refs.[2, 3, 4] (see [3] in Fig.5 (Eq.(17) in section 1)) among other properties also the relative conduction intervals of the valves are influenced (cf. Eq.(36)). E.g., there follows for transistor T2

$$\alpha_{T2}(\varphi_U) = \frac{1}{2} + \frac{M_1}{2} \cos \varphi_U - \frac{M_3}{2} \cos 3\varphi_U \quad (44)$$

This means that in any case a corresponding change of the conduction losses can be expected. The evaluation of Eq.(40) under consideration of Eqs.(39) and (44) leads to

$$P_{F,T2} = \frac{U_{F,T} \hat{I}_N}{2} \left[\frac{1}{\pi} + \frac{M_1}{4} \cos \varphi \right] + r_{F,T} \hat{I}_N^2 \left[\frac{1}{8} + \frac{M_1}{3\pi} \cos \varphi - \frac{M_3}{15\pi} \cos 3\varphi \right] \quad (45)$$

and

$$P_{F,D1} = \frac{U_{F,D} \hat{I}_N}{2} \left[\frac{1}{\pi} - \frac{M_1}{4} \cos \varphi \right] + r_{F,D} \hat{I}_N^2 \left[\frac{1}{8} - \frac{M_1}{3\pi} \cos \varphi + \frac{M_3}{15\pi} \cos 3\varphi \right] \quad (46)$$

($M_3 = 0.25M_1$ for optimized PWM (cf. section 1)). The part of the loss which is dependent on the constant conduction voltage representation therefore is not influenced by the modulation method modification (cf. Eqs.(41) and (43)); the part linked to the conduction resistance is influenced only marginally. As can be considered, e.g., graphically in a simple way (cf. Fig.8), we can write

$$\int_{-\pi}^{\pi} \cos[(2k+1)\varphi_U] \cos[\varphi_U + \varphi] d\varphi_U = 0 \quad k = 1, 2, \dots \quad (47)$$

Therefore in general for a change of the simple sinusoidal modulation method by odd order harmonics or, in general, by a zero quantity m_0 defined by

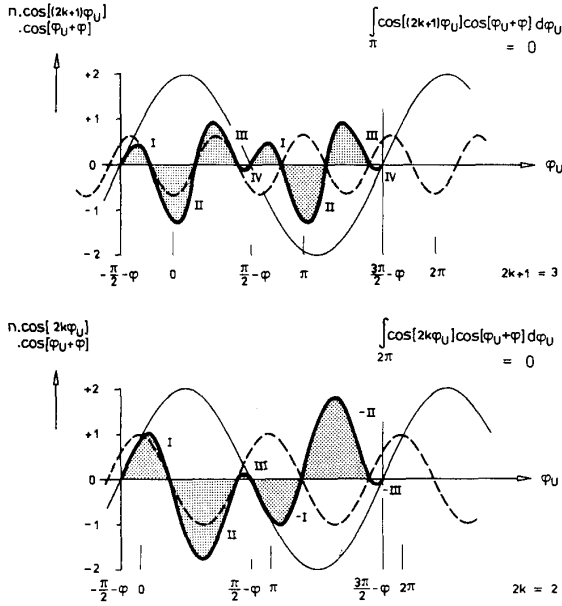


Fig. 8: For derivation of Eq. (47).

Eq. (35) (see modulation methods [2], [3], [4], [5], [6] and [7] in Fig. 5) the conduction losses linked to the not current dependent part of the conduction voltage are not influenced. This means that the calculation can be restricted to the second loss part; as a closer investigation of the modulation methods described in section 1 shows, this power loss contribution can always be approximated with an accuracy which is sufficient for dimensioning purposes via the expression resulting for sinusoidal modulation. The thermal dimensioning of the power electronic devices regarding global conduction losses therefore is only marginally influenced by the shape of the modulation function.

3 Calculation of the Switching Losses

For the calculation of the switching losses related to the modulation methods considered one assumes (according to the measurement results of, e.g., Refs. [8, 9, 10, 11]) a linear dependency of the switching energy loss (appearing for one switching cycle of a bridge leg) on the switched current

$$w_{P,T} \{i_T(\omega NT)\} = k_{1,T} i_T(\omega NT) \quad (48)$$

For the definition of a local switching loss (related to a position of a pulse interval) one can write

$$P_{P,T} = w_{P,T} f_P \quad (49)$$

when a high pulse number is implied.

Averaging

$$P_{P,T2} = \frac{1}{2\pi} \int_{-\pi/2-\varphi}^{+\pi/2-\varphi} P_{P,T2}(\varphi_U) d(\varphi_U) \quad (50)$$

of this switching loss appearing within the positive (or negative) output current half period leads for "continuous" modulation (e.g., sinusoidal modulation [1] or [2] or [3] in Fig. 5, respectively) to a global switching loss of a transistor-diode-pair of a bridge leg (e.g., T_2 and D_1 in Fig. 7)

$$P_{P,T2,D1} = \hat{I}_N f_P \frac{k_{1,T,D}}{\pi} \quad (51)$$

with

$$k_{1,T,D} = k_{1,T} + k_{1,D} \quad (52)$$

The shape of the modulation function basically influences the switching losses only if the various bridge legs are not pulsed within the entire fundamental period with pulse frequency ("discontinuous" modulation, modulation methods [4], [5], [6] and [7] in Fig. 5). As Figs. 9, 10 show then there has to be decided among different cases in dependency on the phase relationship between the fundamentals of the output phase voltage and current. For the switching losses there follows

$$\begin{aligned} P_{P,T2,D1,[4]} &= \frac{\hat{I}_N k_{1,T,D} f_P [4]}{\pi} \left[1 - \frac{(\sqrt{3}-1)}{2} \cos \varphi \right] & \varphi \in [0, \frac{\pi}{6}] \\ &= \frac{\hat{I}_N k_{1,T,D} f_P [4]}{\pi} \left[\sin \varphi + \cos \varphi \right] & \varphi \in [\frac{\pi}{6}, \frac{\pi}{3}] \\ &= \frac{\hat{I}_N k_{1,T,D} f_P [4]}{\pi} \left[1 - \frac{(\sqrt{3}-1)}{2} \sin \varphi \right] & \varphi \in [\frac{\pi}{3}, \frac{\pi}{2}] \end{aligned} \quad (53)$$

$$\begin{aligned} P_{P,T2,D1,[5]} &= \frac{\hat{I}_N k_{1,T,D} f_P [5]}{\pi} (1 - \frac{1}{2} \cos \varphi) & \varphi \in [0, \frac{\pi}{3}] \\ &= \frac{\hat{I}_N k_{1,T,D} f_P [5]}{\pi} \frac{\sqrt{3} \sin \varphi}{2} & \varphi \in [\frac{\pi}{3}, \frac{\pi}{2}] \end{aligned} \quad (54)$$

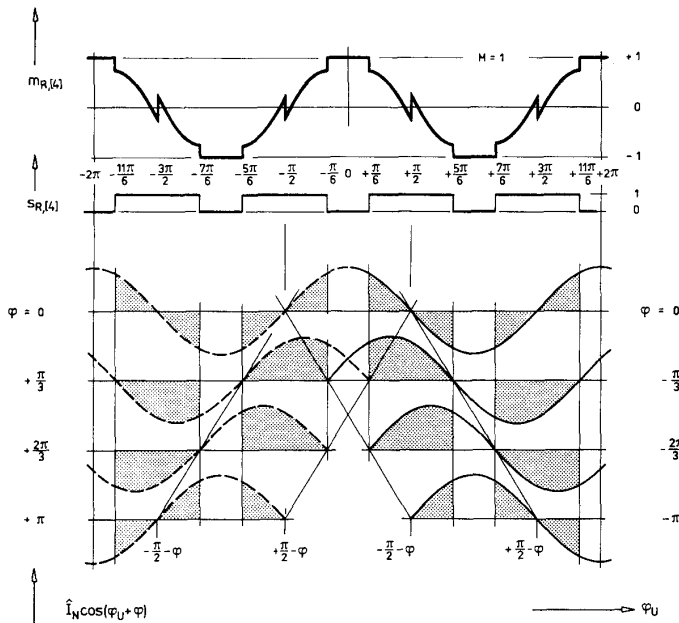


Fig. 9: For derivation of the switching loss dependency on the phase shift between output voltage and output current for modulation method [5] ($m_{R,[5]}$: phase modulation function (given for phase R); $s_{R,[5]}$: switching frequency status of the bridge leg ($s_{R,[5]} = 1$ for switching bridge leg, $s_{R,[5]} = 0$ for intervals when bridge leg is clamped); lower curves: distinction of different cases for the phase angle regions of the output current).

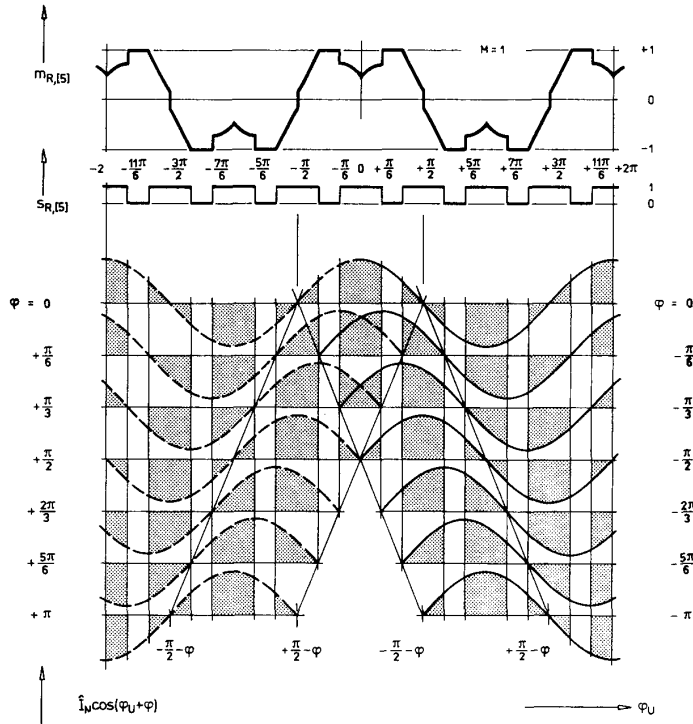


Fig.10: For derivation of the switching loss dependency on the phase shift between output voltage and output current for modulation method [4] ($m_{R,[4]}$: phase modulation function (given for phase R); $s_{R,[4]}$: switching frequency status of the bridge leg ($s_{R,[4]} = 1$ for switching bridge leg, $s_{R,[4]} = 0$ for intervals when bridge leg is clamped); lower curves: distinction of different current cases for the phase angle regions of the output current).

(values for the other phase angle regions follow via symmetry considerations (cf. Figs.9,10 and 11)). Dependent on the phase angle of the output current and on the modulation method used ([4] or [5]) this makes possible (cf. Fig.11) an increase of the "local"² pulse frequency ($f_{P,[4]}$ or $f_{P,[5]}$, respectively) by a factor of

$$\begin{aligned}
 k_{f,[4]} = \frac{f_{P,[4]}}{f_P} &= \frac{1}{\left[1 - \frac{(\sqrt{3}-1)}{2} \cos \varphi\right]} & \varphi \in \left[0, \frac{\pi}{6}\right] \\
 &= \frac{2}{\left[\sin \varphi + \cos \varphi\right]} & \varphi \in \left[\frac{\pi}{6}, \frac{\pi}{3}\right] \\
 &= \frac{1}{\left[1 - \frac{(\sqrt{3}-1)}{2} \sin \varphi\right]} & \varphi \in \left[\frac{\pi}{3}, \frac{\pi}{2}\right]
 \end{aligned} \quad (55)$$

$$\begin{aligned}
 k_{f,[5]} = \frac{f_{P,[5]}}{f_P} &= \frac{1}{\left(1 - \frac{1}{2} \cos \varphi\right)} & \varphi \in \left[0, \frac{\pi}{3}\right] \\
 &= \frac{2}{\sqrt{3} \sin \varphi} & \varphi \in \left[\frac{\pi}{3}, \frac{\pi}{2}\right]
 \end{aligned} \quad (56)$$

There equal global switching loss is assumed as for the case of the simple sinusoidal modulation for which we have equality of "local" and "global" pulse frequency f_P . The shift between the periods where no pulsing of a bridge leg takes place and the associated current fundamental has essential influence on the possible frequency increase. This is true because the calculation of the switching losses (cf. Eqs.(49), (50)) is performed by weighting the instantaneous output current value by the local pulse frequency. If a converter phase is clamped to a bus bar voltage within $\pi/3$ wide intervals (e.g.,

cf. Eqs.(31), (33) or [4], [5] in Fig.5, respectively) then k_f shows a significant dependency on the phase shift of the output current. If the clamping interval of a phase (i.e., there appear no local switching losses) lies symmetrically to the current maximum ($\varphi = 0$), as this is the case for modulation method [5], the local switching frequency can be increased by a factor 2 as compared to continuous modulation. The frequency increase of $k_f = 1.5$ which could be concluded from a superficial consideration of the problem (independent of the current phase angle, see section 1) therefore does not represent the maximum achievable value. However, there appear phase angle regions, where the clamping states will be located in the neighborhood of the current zero crossings ($\varphi = \pi/2$). Then the switching of the bridge legs occurs at high current levels (near or at the current maximum). The possible frequency increase in this case will be given by $k_f \leq 1.5$. If the clamping states are distributed more evenly over the fundamental period, there results - as immediately clear from the previous considerations - a less pronounced dependency of the frequency increase on the current phase shift (cf. [4] Fig.5, or Fig.11, respectively).

A closer discussion of the discontinuous modulation methods [6] and [7] (cf. Fig.5) defined in section 1 by Eqs.(26) and (28) can be omitted here because the frequency increase which becomes possible when these methods are applied can be derived directly from the relationships calculated for modulation method [5]. This becomes immediately clear by comparing [5], [6] and [7] in Fig.5. We have

$$k_{f,[6]}(\varphi) = f_{P,[5]}(\varphi - \frac{\pi}{6}) \quad (57)$$

or

$$k_{f,[7]}(\varphi) = f_{P,[5]}(\varphi + \frac{\pi}{6}) \quad (58)$$

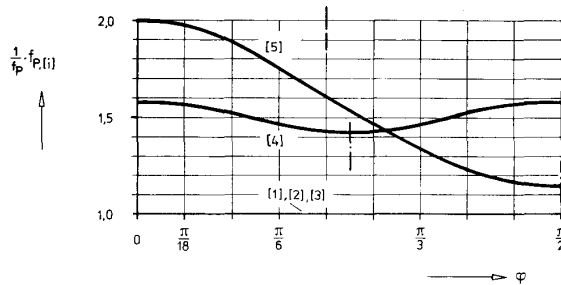


Fig.11: Possible frequency increase $k_{f,[i]}$ of the modulation methods [4] and [5] in comparison to "continuous" modulation methods (e.g., simple sinusoidal modulation [1]) for equal switching losses (as side condition for giving equal bases for comparison purposes).

²The local pulse frequency $f_{P,[i]}$ in this section is given by either $f_P = 0$ for the clamping intervals or by $f_P = f_{P,[i]} = \text{constant}$ for the other time intervals of the fundamental period. For further methods concerning the "modulation" of the pulse frequency see section 4

According to the application area of the PWM converter system (phase angle region) the calculations performed give a criterion for selecting the modulation method to be applied. For the application to AC motor drives, e.g., modulation method [4] would be more advantageous than [5]. The reason is that then according to Eq.(32) and Eq.(34) in the whole modulation region for a phase angle region from 40° to 120° (or -40° to -120°) the harmonic losses of [4] are below the harmonic losses of [5].

4 Optimal Modulation of the PWM Converter Frequency

The optimization of the continuous modulation can be reduced (as described in section 1) to a minimization of the local harmonic current rms value (cf. Eq.(15))

$$\Delta i_{N,RST,rms}^2 = \Delta i_{N,RST,rms,1}^2 + \Delta i_{N,RST,rms,2}^2 \quad (59)$$

$$\begin{aligned} \frac{1}{\Delta i_n^2} \Delta i_{N,RST,rms,1}^2 &= \frac{48}{9} \delta_7 \left\{ \delta_2 \delta_6 (\delta_2 - \delta_6) - 2\delta_{26} [1 - (\delta_7 + \delta_6 + \delta_2)] \right\} \\ \frac{1}{\Delta i_n^2} \Delta i_{N,RST,rms,2}^2 &= \frac{16}{9} \left\{ 6\delta_{26}^2 + 2\delta_{26} - 4\delta_2^4 - 4\delta_6^4 - 4\delta_2 \delta_{26} - 4\delta_6 \delta_{26} - \right. \\ &\quad \left. - 8\delta_2 \delta_6 \delta_{26} + 2\delta_2 \delta_6^2 - \delta_2^2 \delta_6 + 3\delta_6^2 \delta_2 - \delta_2^2 \delta_6^2 \right\} \end{aligned} \quad (60)$$

with

$$\delta_{26} = \delta_2^2 + \delta_2 \delta_6 + \delta_6^2 \quad (61)$$

and

$$\begin{aligned} \delta_6 &= \frac{\sqrt{3}M}{2} \sin\left(\varphi_U + \frac{\pi}{3}\right) \\ \delta_2 &= \frac{\sqrt{3}M}{2} \sin\left(\varphi_U - \frac{\pi}{3}\right). \end{aligned} \quad (62)$$

For the sake of simplicity in the following we only want to refer to the suboptimal solution (cf. Eq.(22) or [2] in Fig.5, respectively)

$$\delta_{7,[2]} = \frac{1}{2} [1 - (\delta_2 + \delta_6)]. \quad (63)$$

The dependency of the optimized local harmonic current rms value on the modulation depth and phase φ_U of the converter voltage space vector is shown in Fig.12. The characteristic shape of the global harmonic losses is given in Fig.6 (cf. [2]). Figure 12 shows a pronounced maximum in the upper modulation region in the vicinity of $\varphi_U = \pi/2$. Therefore one has to raise the question whether or how for a given modulation depth M the shape

of the harmonic power losses can be smoothened and thereby possibly the global harmonic power losses further reduced. The only remaining degree of freedom of the modulation method there is given by the variation of the pulse frequency which has been assumed constant (independently of φ_U) so far. Accordingly the pulse frequency is to be increased in the region $\varphi_U \approx \pi/2$ and can be decreased in the regions $\varphi_U \approx \pi/3$ and $2\pi/3$.

The optimization of the pulse frequency shape $f_{P,FM}(\varphi_U)$ is expressed by a quality functional which has to be minimized

$$I = \frac{1}{\Delta i_n^2} \int_{\frac{\pi}{3}}^{\frac{2\pi}{3}} \frac{1}{k_{f,FM}^2(\varphi_U, M, \varphi)} \Delta i_{N,RST,rms}^2(\varphi_U, M) d\varphi_U \rightarrow \min. \quad (64)$$

The associated side condition is given by keeping the switching losses constant as they result for constant pulse frequency f_P , according to

$$\frac{1}{2\pi} \int_{-\frac{\pi}{2}}^{\frac{\pi}{2} - \varphi} k_1 k_{f,FM}(\varphi_U, M, \varphi) f_P i_{N,R}(\varphi_U, \varphi) d\varphi_U = f_P \frac{k_1 \hat{I}_N}{\pi}. \quad (65)$$

This means equal thermal stress on the power semiconductor devices. According to Eq.(65) the phase shift between converter output current and converter voltage again influences the determination of the switching losses, as already discussed in section 3. (The discontinuous modulation discussed there basically represents a special case of the general frequency modulation treated here). Therefore the optimization has to be performed for each phase angle φ and for each modulation depth M . The side condition (Eq.(65)) can be also written as

$$\int_{\frac{\pi}{3}}^{\frac{2\pi}{3}} k_{f,FM}(\varphi_U, M, \varphi) \zeta(\varphi_U, \varphi) d\varphi_U = 2 \quad (66)$$

with

$$\zeta(\varphi_U, \varphi) = |\cos(\varphi_U + \varphi)| + |\cos(\varphi_U + \varphi - \frac{\pi}{3})| + |\cos(\varphi_U + \varphi + \frac{\pi}{3})|. \quad (67)$$

The weighting function ζ characterizing the influence of the sinusoidal current phase shift is shown in Fig.13.

In general the optimization problem treated here represents a problem of variational calculus: one has to calculate the shape of the relative (local) pulse frequency (the extremal)

$$k_{f,FM} = \frac{1}{f_P} f_{P,FM} = k_{f,FM}(\varphi_U, M, \varphi) \quad (68)$$

(for given M and φ) which minimizes the global harmonic power losses

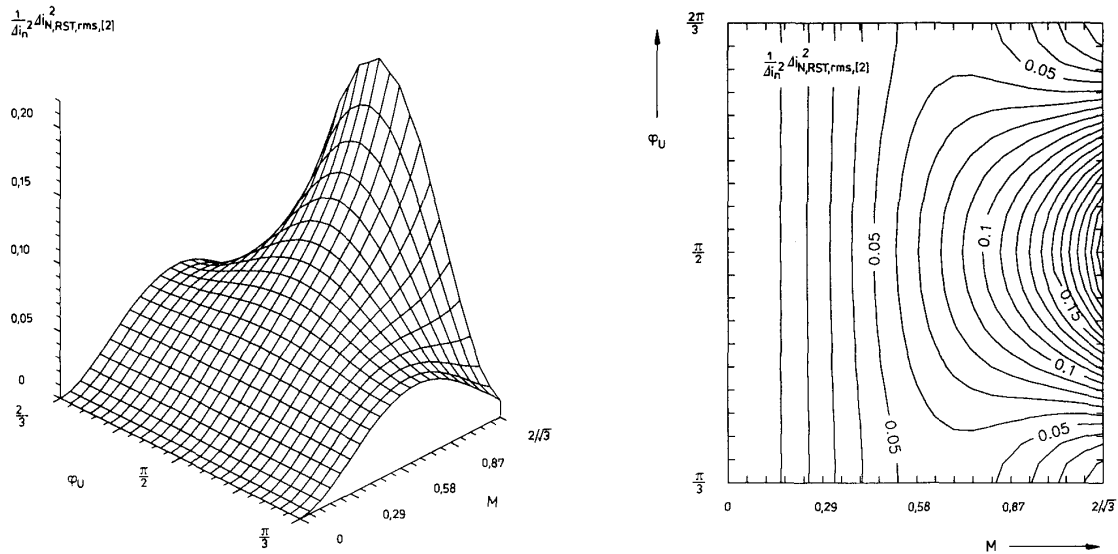


Fig.12:Dependency of the normalized local harmonic power losses $\Delta i_{N,RST,rms}^2$ of the PWM converter system on the position φ_U of the converter voltage space vector and on the modulation depth M for suboptimal modulation [2] (Eqs.(22), (61) and (62) has to be applied to Eq.(59)).

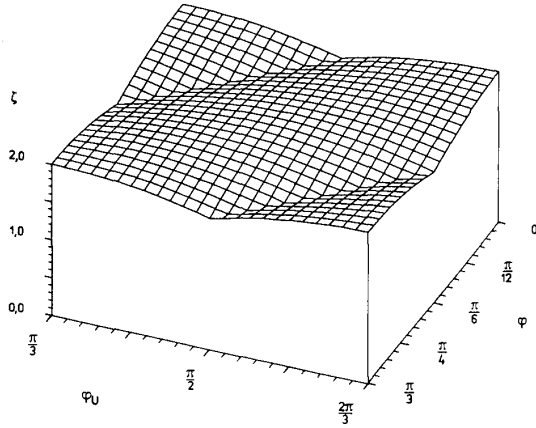


Fig.13:Weighting factor ζ of the normalized local pulse frequency $k_{f,FM}$ for calculating the converter switching losses in dependency on the phase angle φ and on the angle φ_U (cf. Eq.(67)). Due to the symmetries of a purely sinusoidal balanced three-phase system the considerations can be limited to the interval $\varphi \in [0, \pi/3]$.

$\Delta I_{N,rms}^2(M, \varphi)$ where the side condition of constant switching losses is fulfilled. As a necessary condition for obtaining the extremal one can give

$$\frac{\partial}{\partial k_{f,FM}} \left\{ \frac{1}{k_{f,FM}^2(\varphi_U, M, \varphi)} \frac{1}{\Delta i_n^2} \Delta i_{N,RST,rms}^2(\varphi_U, M) + \lambda k_{f,FM}(\varphi_U, M, \varphi) \zeta(\varphi_U, \varphi) \right\} = 0 \quad (69)$$

according to the Euler-Lagrange differential equation of variational calculus. The side condition given as integral is linked to the calculation by the Lagrange multiplier λ . (As known, this parameter is finally determined by inserting of the extremal into the side condition (cf. Ref.[12]).) For the optimal frequency modulation there follows

$$k_{f,FM}(\varphi_U, M, \varphi) = \frac{2 \sqrt[3]{\frac{1}{\zeta(\varphi_U, \varphi)} \Delta i_{N,RST,rms}^2(\varphi_U, M)}}{\int_{\pi/3}^{2\pi/3} \sqrt[3]{\zeta^2(\varphi_U, \varphi) \Delta i_{N,RST,rms}^2(\varphi_U, M)} d\varphi} \quad (70)$$

(cf. Figs.14 and 15). The necessary frequency sweep of the modulation is increased with increasing modulation depth and shows essentially a shape as already expected in the previous discussion. For a practical realization this frequency shape (in first approximation independent of the phase shift φ) can be approximated, e.g., by a simple sinusoidal or triangular modulation

which is only dependent on M . The global harmonic power losses resulting for optimal frequency modulation are given in Fig.16. One has to point out especially the dependency on φ ; there is obtained no essential improvement of the modulation method [2] (constant pulse frequency), however. (Modulation method [2] is treated here as representative case; the other methods should show an equivalent result. This will be treated in more detail in a future paper.)

If one considers (besides the resulting harmonic power losses) also the resulting noise of, e.g., an electric motor supplied by the converter, then the frequency modulation shows significant advantages as compared to a modulation method with constant pulse frequency. This results from the fact that the harmonics (which are concentrated in the immediate vicinity of multiples of the switching frequency for constant pulse frequency) are now distributed in frequency bands of the width

$$B \approx 2f_p(k_{f,FM} - 1). \quad (71)$$

Due to the equal spectral power (as known, the spectral power is not influenced by frequency modulation) their amplitudes are decreased accordingly. There the envelope of these spectral components for a large frequency sweep is defined by the shape of the modulating signal. There follows, e.g., for triangular modulation an almost constant amplitude for the spectral components in the frequency regions defined by Eq.(71).

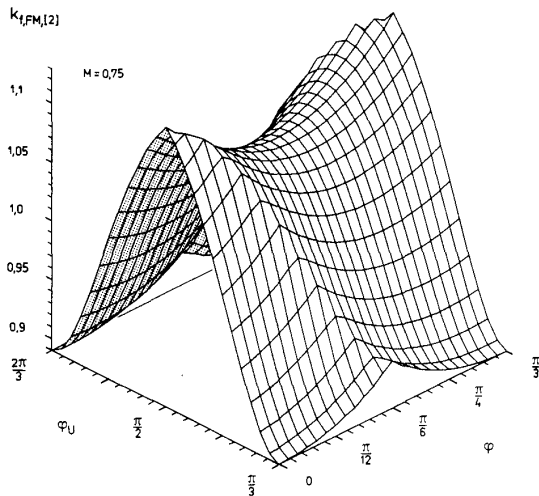
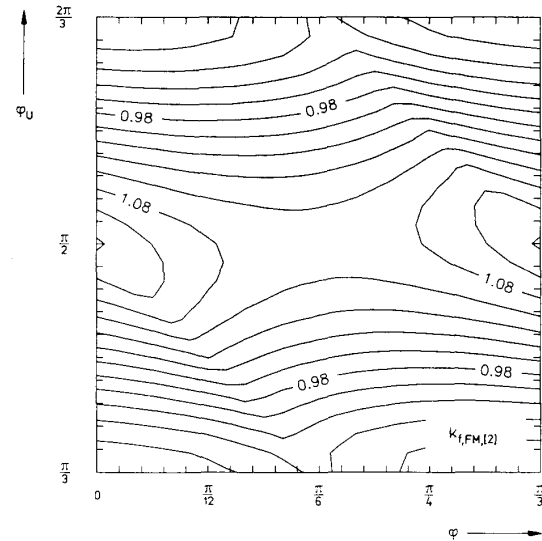


Fig.14:Dependency of the optimal normalized frequency $k_{f,FM[2]}$ of the pulse frequency modulation on the position $\varphi_U \in [\pi/3, 2\pi/3]$ of the converter voltage space vector and on the phase shift φ (referred to φ_U) of the converter output current; $M = 0.75$ (cf. Eq.(70)).



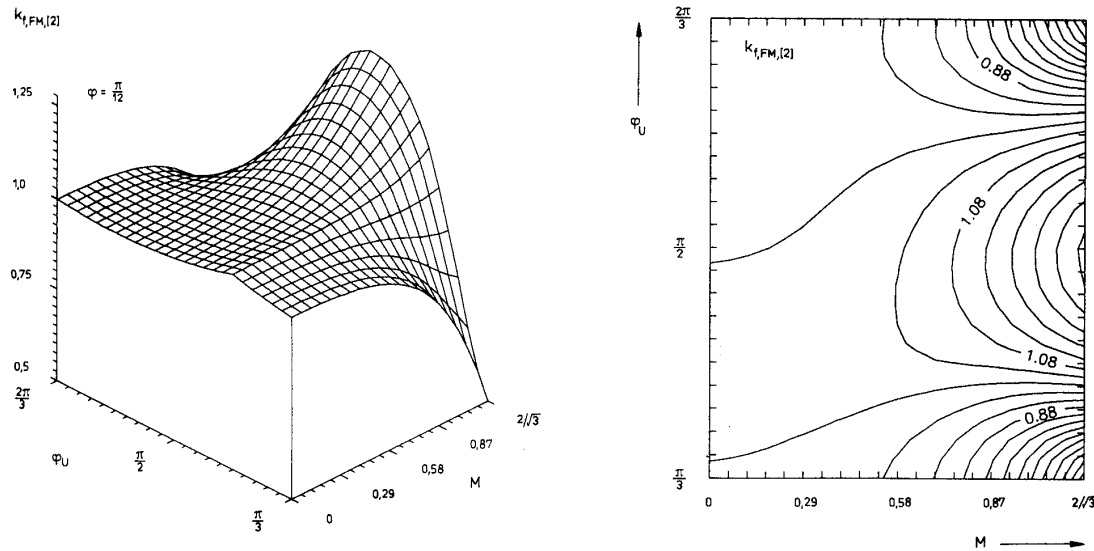


Fig.15: Dependency of the optimal normalized frequency $k_{f,FM}$ of the pulse frequency modulation on the position $\varphi_U \in [\pi/3, 2\pi/3]$ of the converter voltage space vector and on the modulation depth M ; $\varphi = 0$ (cf. Eq.(70)).

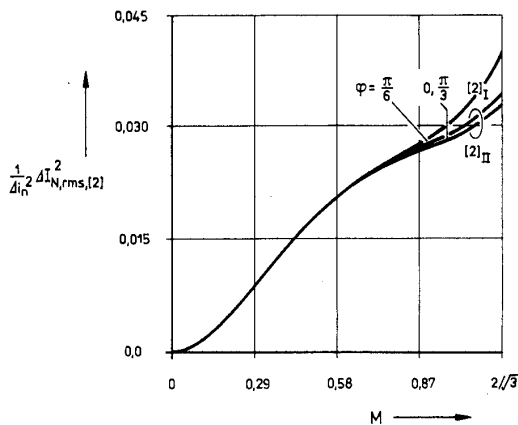


Fig.16: Comparison of the normalized global harmonic losses of one phase for constant (denoted by $[2]_I$) and modulated (denoted by $[2]_{II}$) converter pulse frequency. The comparison is made for equal switching losses in both cases to give a common basis for the comparison. (Parameter of the family of curves: phase angle φ of the output current).

The resulting noise of the AC motor supplied by a PWM converter therefore is distributed in a wider frequency band as compared to modulation methods with constant pulse frequency. There do not appear pronounced audible frequencies with multiples of the pulse frequency. A detailed investigation of this problem area will be the topic of a paper being in preparation.

5 Conclusions

The main topic of this paper is the determination of those power loss components of a PWM converter system which can be (besides the harmonic losses) influenced by the modulation method selected. Those power loss components are usually neglected in pulse pattern optimization methods known from the literature because the optimization is performed with the side condition of

a given average (global) switching frequency, but not with the essential side condition of defined global switching losses.

If the assumption of sufficient thermal inertia of the power semiconductor devices is not fulfilled anymore (meaning low output frequencies) one has to include a dynamic thermal model (transient thermal resistance) for the power electronic devices for considering the device behavior with respect to the switching and conduction losses within the fundamental period. A pulse pattern optimization then would be thinkable, e.g., with the side condition of a maximum allowable chip temperature.

For the optimization of the stationary behavior of an AC motor drive system (which is the final goal of a pulse pattern optimization) one in general should check if a detailed modelling limited only to the motor is sufficient. One has to consider rather also the loss contributions mentioned in this paper and therefore especially the converter losses. It would be not advisable to optimize a few percent of harmonic motor power losses (which are small for high pulse frequencies in any case) if one would not consider the possibly (much) higher influences on the losses of the converter due to the nonideality of the power electronic devices.

References

- [1] Halász, S.: *Voltage Spectrum of Pulse-Width-Modulated Inverters*. Technical University Budapest, Periodica Polytechnica, Electrical Engineering, Vol.25, No.1, 135-145 (1981).
- [2] Kolar, J. W., Ertl, H., and Zach, F. C.: *Analytically Closed Optimization of the Control Method of a PWM Rectifier System with High Pulse Rate*. Proceedings of the PCIM'90, Munich, June 27-29 (1990).
- [3] Bowes, S. R., and Midoun, A.: *Suboptimal Switching Strategies for Microprocessor-Controlled PWM Inverter Drives*. IEE Proceedings, Vol. 132, Pt. B, No. 3, 133-148 (1985).
- [4] Buja, G., and Indri, G.: *Improvement of Pulse Width Modulation Techniques*. Archiv für Elektrotechnik 57, 281-289 (1977).
- [5] van der Broeck, H. W., Skudelny, H. C., and Stanke, G. V.: *Analysis and Realization of a Pulsewidth Modulator Based on Voltage Space Vectors*. IEEE Transactions on Industry Application, Vol. IA-24, No.1, 142-150 (1988).
- [6] Ikeda, Y., Itsumi, J., and Funato, H.: *The Power Loss of the PWM Voltage-Fed Inverter*. 19th PESC '88 Record, Kyoto, Japan, April 11-14, Vol.1, 277-283 (1988).

- [7] **Nishizawa, J., Tamamushi, T., and Nonaka, K.:** *The Experimental and Theoretical Study on the High Frequency and High Efficiency SI Thyristor Type Sinusoidal PWM Inverter.* Proceedings of the 14th PCF'87 Conference, Long Beach, CA, Sept. 14-17, 167-181 (1987).
- [8] **Kolar, J. W., Ertl, H., and Zach, F. C.:** *Calculation of the Passive and Active Component Stress of Three-Phase PWM Converter Systems with High Pulse Rate.* Proceedings of the 3rd European Conference on Power Electronics and Applications, Aachen, Oct. 9-12, Vol. 3, 1303-1311 (1989).
- [9] **Mestha, L. K., and Evans, P. D.:** *Optimization of Losses in PWM Inverters.* IEE Conference Publication, No. 291, 394-397 (1988).
- [10] **Rockot, J. H.:** *Losses in High-Power Bipolar Transistors.* IEEE Transactions on Power Electronics, Vol. PE-2, No. 1, 72-80 (1987).
- [11] **Sneyers, B., Lataire, Ph., Maggetto, G., Detemmerman, B., and Bodson, J. M.:** *Improved Voltage Source GTO Inverter with New Snubber Design.* 2nd European Conference on Power Electronics and Application, Grenoble, France, Sept. 22-24, Vol.1, 31-36 (1987).
- [12] **Zach, F.:** *Technisches Optimieren.* Vienna - New York: Springer Verlag, 1974.

The authors are very much indebted to the Austrian Fonds zur Förderung der wissenschaftlichen Forschung which supports the work of the Power Electronics Section at their university.